

Model calculation of nitrogen properties in III-V compounds

B. Gil, J. P. Albert, J. Camassel, and H. Mathieu

Groupe d'Etude des Semiconducteurs, Université des Sciences et Techniques du Languedoc, F-34060 Montpellier Cédex, France

C. Benoit à la Guillaume

Groupe de Physique des Solides de l'Ecole Normale Supérieure, Tour 23, 2 place Jussieu, F-75251 Paris Cédex 05, France

(Received 15 July 1985)

We present a semiphenomenological model calculation of the nitrogen-related traps in GaP and related compounds. Working in the one-band—one-site approximation, the complex character of the lowest conduction band is taken into account by using the model density of states previously introduced by Kleiman. In the case of NN pairs in GaP, this results in different series of levels whose energy position depends on structure factors which couple the nitrogen-nitrogen relative positions in real space and the extrema of the conduction band in \mathbf{k} space. A tentative identification of these levels is done, in the light of the present calculation, by taking account of the experimentally determined symmetry. A comparison is next performed with recent hydrostatic stress experiments and with the pair dependence of the local-field parameter which splits the Γ_8 bound hole. Concerning isolated nitrogen, the model predicts composition and pressure dependences in very good agreement with experimental results in $\text{Ga}_x\text{In}_{1-x}\text{P}$, $\text{GaAs}_{1-x}\text{P}_x$ or GaAs.

I. INTRODUCTION

In spite of considerable theoretical and experimental interest, the understanding of isoelectronic traps in semiconductors is still far from complete. The best example is nitrogen in gallium phosphide.¹ In the concentration range $N < 10^{17} \text{ cm}^{-3}$, nitrogen acts as an isolated electron trap which behaves like a deep center.² The corresponding binding energy is, however, vanishingly small^{3,4} and the exciton binding energy ($\sim 11 \text{ meV}$) is only understood in terms of exchange and correlation effects. In the concentration range $N > 10^{17} \text{ cm}^{-3}$, a second series of traps appears deeper in the forbidden band. The corresponding centers are pairs of nitrogen atoms. A conventional model, first proposed by Thomas and Hopfield¹ associates the deeper state NN_1 with two nitrogen atoms in first-neighbor position on the anionic sublattice; then NN_2 would correspond to the second-neighbor position, and so on. This natural viewpoint is supported in part by standard model calculations⁴ made in the framework of the effective-mass theory, which, however, ignores the multivalley structure of the conduction band in GaP. In fact, the only two (to our knowledge)^{5,6} elaborate calculations which have explicitly taken into account this complex aspect of the conduction band show that rather intricate interference effects due to the presence of equivalent minima in the Brillouin zone severely affect the position of the pair levels and that this simple natural ordering is lost.

In the preceding paper,⁷ hereafter referred to as paper I, we have presented an investigation of the real-space orientation of nitrogen-nitrogen (NN) pairs in GaP. Applying a series of uniaxial stress in order to lower the crystal symmetry, we could deduce in turn the symmetry properties of pairs ranging from NN_1 to NN_7 . We came to the conclusion that the standard assignment could not stand up to experimental results and should be reinvestigated to

account for the new experimental findings. It is the purpose of the present work to provide us with a semiphenomenological model calculation which keeps all the basic ingredients of the problem—e.g., the short-range nature of the nitrogen perturbative potential and the multivalley structure of the conduction band of GaP—but stays simple enough to be extended to the analysis of the experimental data under external perturbations. Although such an oversimplified model cannot be expected to give absolute energies for the pair recombination lines directly comparable to the experimental data, it will be helpful in clarifying the relative influence of the interference effects due to the presence of several principal and subsidiary minima in the Brillouin zone. On the basis of the resulting ordering of the levels and of the experimentally found pair symmetry, a tentative identification of the levels origin will be discussed. Since the multivalley structure of the conduction band in GaP strongly affects the position in energy of the pair levels and their pressure dependence, the results of our model will be checked versus hydrostatic pressure and alloy composition in $\text{Ga}_x\text{In}_{1-x}\text{P}$ and $\text{GaAs}_{1-x}\text{P}_x$. The behavior under hydrostatic pressure of the N level in GaAs will lastly be considered in the light of recent experimental data.

II. SPECIFICITIES OF THE PROBLEM

A correct description of the binding mechanism of excitons bound to isoelectron centers has deserved considerable attention during the last twenty years.⁸ Focusing only on nitrogen in GaP, the most important points are the following.

(i) Hopfield, Thomas, and Lynch⁹ (HTL) introduced the very workable concept of isoelectronic donors and acceptors. According to this simple viewpoint, nitrogen in GaP

is an isoelectronic acceptor. It introduces a bound state for the electron which next binds a hole by Coulomb interaction. Although its binding energy is very weak, this bound-electron level possesses the characteristics of a "deep-impurity state" because of the localized nature of the impurity potential.² Such a viewpoint is partly supported by luminescence excitation spectroscopy in the case of deep NN pairs.¹⁰ On the other hand, assuming that the potential of the substitutional impurity is nothing but the difference between the bare atomic (pseudo) potentials of nitrogen and phosphorus, Faulkner performed a pioneering calculation.⁵ Developing the bound state over the two lower conduction bands, he ended up with a binding energy of the order of 1 eV, which is two orders of magnitude larger than the exciton binding energy (~ 10 meV).

(ii) Discussing the weakness of this approach, both Phillips¹¹ and Allen¹² suggested that the lattice deformation around the impurity should play an important part in the binding mechanism. Indeed, recent Green's-function calculations proved that significant results could be achieved by taking into account the multiband nature of the level¹³ and by using a more realistic medium-range potential⁶ but, although the position of the bound-electron level was found to be more realistic than the one formerly obtained by Faulkner, more progress in this direction seems yet to be rather difficult. This is because of the formidable task of incorporating properly lattice relaxation as well as electronic polarization and multielectronic correlations in a multiband self-consistent calculation.^{14,15}

(iii) Coming now to the problem of NN pairs in GaP, a simplified non-self-consistent approach is usually adopted in which the whole perturbation is obtained as the superposition of two identical model potentials adjusted to describe properly the isolated impurity. In this way both Faulkner,⁵ on the one hand, and Brand and Jaros,⁶ on the other, report a satisfactory agreement with experimental data as far as the energy range of pairs spectra is concerned (~ 0 –150 meV). However, their resulting sequence of levels differ with each other and also with the conventional assignment.

It is the purpose of the present work to check how far a simple calculation can lead when dealing with nitrogen pairs. Similar paths along this line have been already followed by Hsu *et al.*¹⁶ and by Kleiman,¹⁷ but were mostly restricted to isolated nitrogen. In this work we perform a Slater-Koster-type model calculation which takes into account the indirect structure of the lowest conduction band in GaP. We find that different series of levels should appear, depending on the structure factors which couple the nitrogen-nitrogen distances in real space and the extrema of the density of states in k space. Most levels obtained in the calculation correspond with symmetries C_{2v} or C_s and can be associated with the experimental results of paper I. However, some levels appear also in the calculation which do not correspond to existing symmetries. Since similar orderings are found in more elaborate calculations,^{5,6} we do not believe in a systematic discrepancy. These levels should correspond to lines of unidentified symmetry and confirm that lattice-relaxation effects play a very important part in the final description of the complex.

III. BINDING TO NN PAIRS: A ZERO-STRESS CALCULATION

The most general Hamiltonian that describes a bound-exciton state is³

$$H = H_0(e) + V_i(e) + H_0(h) + V_i(h) + V(e, h), \quad (1)$$

where $H_0(e)$ and $H_0(h)$ stand, respectively, for the individual Hamiltonians of the electron and the hole in the absence of one another in the perfect crystal; $V_i(e)$ is the short-range (attractive) impurity potential, associated with pair i , which binds the electron, while $V_i(h)$ is the (repulsive) isoelectronic potential experienced by the hole; $V(e, h)$ denotes the mutual Coulomb and exchange interactions. Let us follow the path of HTL and concentrate on the electron binding energy E_e . This is found by solving the simplified Hamiltonian

$$[H_0(e) + V_i(e)] |\psi\rangle = E_e |\psi\rangle. \quad (2)$$

The localized electron (E_e) behaves like an acceptor and binds a hole with an energy E_I . The binding energy of the exciton is then $E_B = E_e + E_I$. These simplifying assumptions mean that the acceptor binding energy E_I is independent of E_e and that the variations in the exciton binding energies E_B are primarily determined by the electronic part of the perturbation. This has been well established for deep NN_{*i*} pairs.¹⁰ Next, in the light of a perturbative approach it will be interesting to examine the possible dependence of E_I with the configurations of the pairs. This will be done in the following section (Sec. IV), where a comparison between the theoretically and experimentally determined local-field parameter ϵ_1 is made.

In order to simplify the computational work and get an easily tractable model which could be extended to the analysis of external perturbations, we now make the so-called "one-band approximation." This amounts to neglecting the expansion coefficients of the bound state $|\psi\rangle$ on all crystal Bloch states except the lowest conduction band. This can be justified in the light of previous multiband calculations^{5,6} and, because of the small binding energies investigated, should not be a too bad approximation.

A. Model potential

Within this scheme, $H_0(e)$ now describes the lowest conduction band of GaP, while $V_i(e)$ corresponds to the pair potential. Since we just want one single parameter in our semiphenomenological calculation, the best way is to concentrate first on NN _{∞} . This corresponds to the well-known problem of one single nitrogen atom in GaP whose solution is a marginal potential⁴ with a vanishingly small binding energy.³ Expanding $|\psi\rangle$ on the Wannier function of the conduction band, we get the bound state as a solution of the equation

$$\det \|\delta_{nm} - \langle \mathbf{R}_n | G_0(E) U | \mathbf{R}_m \rangle\| = 0, \quad (3)$$

where $|\mathbf{R}_n\rangle$ denotes the conduction-band Wannier function (WF) centered at site \mathbf{R}_n and $G_0(E)$ is the Green's function of the conduction band:

$$G_0(E) = (E - H_0)^{-1}.$$

Written in the WF basis, the matrix elements of the Green's function are

$$\langle \mathbf{R}_n | G_0(E) | \mathbf{R}_m \rangle = \frac{1}{N} \sum_{\mathbf{k}} \frac{e^{i\mathbf{k} \cdot (\mathbf{R}_n - \mathbf{R}_m)}}{E - E(\mathbf{k})}. \quad (4)$$

$E(\mathbf{k})$ is the energy of the Bloch state with wave vector \mathbf{k} , and the sum in (1) has to be extended over all the wave vectors of the first Brillouin zone (BZ). U is a short-range Koster-Slater (KS)-type potential which acts on electrons in the conduction band. In order to check the possible importance of lattice-relaxation effects, we investigated two slightly different models. First a conventional (one-site) KS potential was used. It affects only the site of the impurity and can be easily fitted to give a vanishing binding energy for isolated nitrogen. Next, an "extended" KS-type potential was introduced. It affects both the site of the impurity and the first shell of its nearest (anionic) neighbors. Previous investigations along this line concern isolated N traps in $\text{GaAs}_{1-x}\text{P}_x$ (Ref. 16) and it was found that such a model potential might simulate the strain field surrounding the impurity. In this work we use the same type of medium-range potential to investigate how a more extended perturbation could affect the results obtained with a zero-radius Koster-Slater approximation. It is shown in Ref. 16, that within the energy range of interest here (0–150 meV) and when dealing with the totally symmetric A_1 state which is the most likely to be bound, this extended KS model is formally equivalent to an energy-dependent one-site potential. As a consequence, we shall write the pair potential as

$$V_i = V_0(|\mathbf{0}\rangle\langle\mathbf{0}| + |\mathbf{R}_i\rangle\langle\mathbf{R}_i|), \quad (5)$$

where $\mathbf{0}$ and \mathbf{R}_i indicate the locations in real space of the two N impurities constituting the pair. V_0 is constant in the one-site approximation.

The bound states introduced by the different NN_i pairs are then easily found as solutions of

$$G_0(E) \pm G_0(E, \mathbf{R}_i) = \frac{1}{V_0}, \quad (6)$$

where V_0 produces a bound level with energy^{3,4} $E_0 \simeq 0$ for the isolated impurity (marginal potential):

$$G_0(E_0) = \frac{1}{V_0}.$$

In these expressions, $G_0(E)$ and $G_0(E, \mathbf{R}_i)$ are the diagonal and nondiagonal Green's function given by

$$G_0(E) = \frac{1}{N} \sum_{\mathbf{k}} \frac{1}{E - E(\mathbf{k})}, \quad (7)$$

$$G_0(E, \mathbf{R}_i) = \frac{1}{N} \sum_{\mathbf{k}} \frac{e^{i\mathbf{k} \cdot \mathbf{R}_i}}{E - E(\mathbf{k})}. \quad (8)$$

The plus and minus signs in Eq. (6) correspond, respectively, to the familiar bonding and antibonding molecular states E_{\pm} which lie on either side of E_0 . The k components (i.e., the expansion coefficients on the Bloch functions of the conduction band) of these two states can be, respectively, written as

$$\phi(\mathbf{k}) = AU_0 \left[1 \pm \frac{e^{-i\mathbf{k} \cdot \mathbf{R}_i}}{E_{\pm} - E(\mathbf{k})} \right], \quad (9)$$

where A is a normalization constant. As already noticed by Faulkner, it is clear from Eq. (9) that two different states will exist. States with $\phi(\mathbf{k}=0)=0$ cannot be associated with the direct creation and/or recombination of a bound exciton at $\mathbf{k}=0$. They are said to be dipole forbidden. States with $\phi(\mathbf{k}=0) \neq 0$, on the contrary, are dipole allowed. We shall come back to this point later when discussing the results of the calculation. Let us now define the model density of states used to describe the conduction band.

B. Model density of states

In order to perform reliable comparisons, we have used in this calculation the model density of states already introduced by Kleiman.¹⁷ The BZ is partitioned in regions associated with Γ , X , and L minima around which the energy dispersion of the band $E_i(\mathbf{k})$ is approximated by a parabolic expansion of finite extent. The great advantage of such an approach lies in its ability to describe the multivalley aspect of the conduction band in GaP as well as the change in band structure which appears under hydrostatic and/or uniaxial stress or when alloying GaP with GaAs. This can be done simply by shifting the relative minima Γ , X , and L relative to each other and taking the appropriate effective mass. A full description of the model is given in the Appendix, together with the numerical values affecting the parameters.

In this case, the Green's functions can be expressed as

$$G_0(E) = g_{\Gamma}(E) + 3g_X(E) + 4g_L(E), \quad (10)$$

$$G_0(E, \mathbf{R}_i) = f_{\Gamma}(\mathbf{R}_i)g_{\Gamma}(E, |\mathbf{R}_i|) + f_X(\mathbf{R}_i)g_X(E, |\mathbf{R}_i|) + f_L(\mathbf{R}_i)g_L(E, |\mathbf{R}_i|),$$

where the functions $g_k(E)$ and $g_k(E, |\mathbf{R}_i|)$, corresponding to the three minima Γ , X , and L , are given in the Appendix. All coefficients $f_k(\mathbf{R}_i)$ ($k = \Gamma, X, L$) are structure factors defined by

$$f_k(\mathbf{R}_i) = \sum_{l \in k} e^{i\mathbf{K}_l \cdot \mathbf{R}_i}, \quad (11)$$

where the sum in (11) has to be performed over all non-equivalent minima of type k whose position in \mathbf{k} space is given by \mathbf{K}_l . The important point to outline is that, according to the relative separations \mathbf{R}_i between the two nitrogen atoms, these structure factors take different values. They are listed in Table I.

The nitrogen-nitrogen pairs can now be classified into (2×3) classes, according to the respective values of the $f_k(\mathbf{R}_i)$. Each class is constituted by all \mathbf{R}_i values which have the same set of structure factors. Lastly, since each $g_k(E, |\mathbf{R}_i|)$ is a monotonical function (decreasing with increasing $|\mathbf{R}_i|$), it is readily seen from Eq. (6) that within each class the binding energy of NN impurity levels is a monotonically decreasing function of $|\mathbf{R}_i|$. In other words, within a class, we find the simple physical idea that the closer the impurities the deeper the bound

TABLE I. Structure factors $f_k(\mathbf{R}_i)$ which concern both X and L valleys for several values of the nitrogen separation R . We define R as a function of the components along the elementary cubic axis: $\mathbf{R}_{\alpha\beta\gamma} = (a/2)(\alpha\mathbf{i} + \beta\mathbf{j} + \gamma\mathbf{k})$, with $a = 5.45 \text{ \AA}$.

| $\alpha\beta\gamma$ | $f_X(\mathbf{R}_{\alpha\beta\gamma})$ | $f_L(\mathbf{R}_{\alpha\beta\gamma})$ |
|---------------------|---------------------------------------|---------------------------------------|
| 110 | -1 | 0 |
| 112 | -1 | 0 |
| 002 | +3 | -4 |
| 022 | +3 | +4 |
| 224 | +3 | +4 |
| 222 | +3 | -4 |
| 044 | +3 | +4 |
| 244 | +3 | -4 |
| 123 | -1 | 0 |
| 013 | -1 | 0 |

state. The new point comes from the six different classes introduced by the multivalley structure of the conduction band. The relative ordering of levels which belong to different classes can only be obtained by a numerical calculation.

C. Numerical results and discussion

We have used both the one-site approximation and the multisite nearest-neighbor KS-type potential already discussed. Both were adjusted to give a vanishing binding energy for the isolated N impurity and give energy levels in close agreement. This is shown in Table II. The most striking feature of both calculations is the relative ordering of the levels. Although these energies have the correct order of magnitude when compared with the experimental data of Cohen and Sturge,¹⁰ the pair ordering is at variance with the one predicted by the conventional model. This is a direct consequence of the dependence of the non-diagonal Green's function $G_0(E, \mathbf{R}_i)$ on the direction of \mathbf{R}_i which comes through the structure factors $f_k(\mathbf{R}_i)$. The lowest level does not originate from the nearest-neighbor $\langle 011 \rangle$ pairs as in the conventional model but rather from more distant $\langle 022 \rangle$ pairs. Even more interesting to discuss is the fact that $\langle 110 \rangle$ should not be dipole active. This comes from the influence of the X valleys which greatly outweighs that of L and Γ because of their proximity to the bound levels.

The six classes of pairs previously defined can be regrouped into two families, according to the value of their

TABLE II. Electron binding energies obtained for NN pairs in the calculations using different model potentials.

| Pair | Dipole character at $k=0$ | Unisite calculation | Multisite calculation |
|-------------|---------------------------|---------------------|-----------------------|
| 220 | allowed | 114 | 117 |
| 200 | allowed | 46 | 43 |
| 400 | allowed | 44 | 40 |
| 422 | allowed | 28 | 23 |
| 440 | allowed | 19 | 14 |
| 442 | allowed | 15 | 11 |
| 622 | allowed | 12 | 8 |
| 660 | allowed | 11 | 7 |
| 644 | allowed | 9 | 6 |
| 110 | forbidden | 66 | 64 |
| 211 | forbidden | 19 | 14 |
| 123 | forbidden | 8 | 4 |
| 013 | forbidden | 8 | 4 |
| NN_∞ | allowed | ~ 1 | ~ 1 |

structure factors at point X ($+3$ or -1). $f_X(\mathbf{R}) = +3$ gives only a bound level when the plus sign is inserted in Eq. (6), while for $f_X(\mathbf{R}) = -1$, only the minus sign gives a bound state. Now, it is readily seen from Eq. (9) that in this latter case the $\mathbf{k}=0$ component of the impurity state is null: without the participation of a momentum conservative phonon, we cannot directly create or recombine a bound exciton. Belonging to this family are $\langle 110 \rangle$, $\langle 112 \rangle$, $\langle 123 \rangle$, etc. As previously analyzed by Faulkner,⁵ we emphasize that these striking effects come from the interferences between the contributions of each X minimum to the wave function of the impurity level.

These interferences are a direct consequence of the multivalley structure of the conduction band and of the short-range character of the perturbative potential. This prevents, in our case, the use of the conventional intervalley scattering perturbative approach, as it is often used in the framework of the effective-mass theory. However, in the framework of this theory, it has been effectively shown that such interferences induce a renormalization of the effective potential appearing in the effective-mass equation.¹⁸ In our case, this is the same kind of renormalization which occurs for axial defects, but the renormalization is now orientation dependent.

We perform in Table III a comparison between the

TABLE III. Respective order of levels which have been found by Faulkner (Ref. 5), Jaros and Brand (Ref. 6), and in this work. The deepest pairs with allowed (forbidden) configurations are 220 (110), whatever may be the details of the calculation.

| | | 220 | 200 | 440 | 400 | 422 | 420 | 620 | 600 |
|----------------------------------|-----------|-----|-----|-----|-----|-----|-----|-----|-----|
| Faulkner ^a | allowed | 220 | 200 | 440 | 400 | 422 | 420 | 620 | 600 |
| | forbidden | 110 | 330 | 211 | 550 | 411 | | | |
| Jaros <i>et al.</i> ^b | allowed | 220 | 200 | 400 | 222 | 422 | 440 | 420 | |
| | forbidden | 110 | 411 | 310 | 211 | | | | |
| This work | allowed | 220 | 200 | 400 | 420 | 422 | 440 | 222 | 600 |
| | forbidden | 110 | 211 | 321 | 330 | | | | 442 |

^aReference 5.

^bReference 6.

theoretical ordering found in this calculation and the one obtained by Faulkner⁵ and Brand and Jaros.⁶ There is a striking similarity between our results and those obtained by Brand and Jaros. In the calculation of Brand and Jaros, a sophisticated Green's-function method, involving a ten-band expansion for the defect levels and a model pseudopotential for the N impurity, was used. The model pseudopotential incorporated a short-range attractive part and a medium-range repulsive contribution. In both cases we find the following: provided the isolated N level is adjusted at the conduction-band edge, the $\langle 022 \rangle$ pairs lie at nearly the same energy in both calculations. This together with the close correspondence between the ordering of most energy states led us to feel that our approach (despite its simplicity) retains all the basic ingredients of the problem. The disagreement between the conventional affectation of the levels and the energy scheme found in both theoretical approaches is evident. It can be explained in two different ways.

(i) Either one assumes that a calculation cannot provide reliable informations about the pair problem (this is the standard viewpoint, implicitly adopted up to now), or

(ii) one assumes that the theoretical results might have some significance and use it as a guideline in discussing the experimental data. Of course we know that no theoretical approach can be expected to position the bound states with an accuracy sufficient to allow an unambiguous one-by-one affectation, but we can try to make a tentative identification in terms of local symmetry. In other words, we shall classify all states which are compatible with the results of the calculations and the experimental findings.

The first problem we want to deal with concerns NN_2 . Remember that NN_2 (i) is associated with a very small luminescent intensity, (ii) has never been found in absorption experiments,^{1,19} (iii) exhibits the most important pressure coefficient,²⁰ and (iv) exhibits the larger local-field splitting of the bound hole.¹⁹ We believe that NN_2 is a forbidden pair associated with the two nitrogen atoms in first-neighbor position ($\langle 110 \rangle$ pair).

We emphasize that this assignment does not correspond, in a strict sense, to the result of the calculation (the $\langle 110 \rangle$ states appear too high) or to the local symmetry [we have found a local symmetry (aac) with $a > c$]. These discrepancies certainly come from the relaxation of the lattice around the defect which contributes to making the trap luminescent. It is to be noted here that the existence of theoretically forbidden or allowed transitions previously noted [Eq. (9)] is strictly dependent upon the superposition rule [Eq. (5)] implicitly assumed in constructing the pair potential. Although this rule is presumed to be valid at large separations, the additivity of local strain effects around each impurity (which can be absorbed in the one-site potential at large distance) becomes more and more questionable with decreasing distance. The highest sensitivity of the $\langle 011 \rangle$ pair to hydrostatic pressure could then also be explained by a coupling between the two Wannier functions centered on each impurity via a strain-induced potential.

Concerning NN_1 , we resolved a local C_{2v} symmetry which agrees satisfactorily with the symmetry of the

lower bound state with $\phi(\mathbf{k}=0) \neq 0$. This is $\langle 220 \rangle$, whatever the model calculation is (see Table III). Accordingly we believe that NN_1 is associated with the family of $\langle 220 \rangle$ pairs. NN_4 and NN_7 correspond also with C_{2v} , experimental symmetry, and strongly radiative defects. Similarly, we believe that they should be associated with the next defects of $\langle aa0 \rangle$ symmetry obtained in the calculation. They are $\langle 440 \rangle$ and $\langle 660 \rangle$ pairs, respectively.

Concerning NN_3 , we resolved a C_s local symmetry, and a close consideration of the data suggested $a > c$. Since the pair appears strongly allowed, both in luminescence and absorption spectroscopy, we do not believe in a forbidden configuration. We suggest that NN_3 might be associated with the $\langle 442 \rangle$ pair [which is the pair of lowest energy which appears in the different calculations with (aac) symmetry and $a > c$] or with any configuration similar to $\langle 442 \rangle$.

Concerning NN_5 and NN_6 , we could not resolve any unambiguous splitting patterns and clearly determine the local pair symmetry. However, outlining the preferential sensitivity to $\langle 001 \rangle$ stress which had been noticed, we suggested some possible C_s orientation with $c > a$. Again we emphasize that NN_5 corresponds to strong absorption and luminescence lines: it should not be associated with a forbidden pair. On the other hand, we find in the calculation, two levels ($\langle 002 \rangle$ and $\langle 004 \rangle$) which cannot be simply associated with any experimental result, despite the fact that their calculated binding energy lies in the compatible energy range. The corresponding symmetry does not correspond to any splitting patterns under stress of any investigated pair. We have thus performed several model calculations, slightly varying the parameters in Kleiman's conduction-band model. We have next used another model density of states due to Mariette *et al.*²¹ and even introduced anisotropic masses at point X. Every time we find the same ordering for the lowest level, which indicates a strong insensitivity to the details of the model used. Keeping in mind the oversimplification of our model, which does not include long-range strain or polarization effects and involves an oversimplified conduction-band model, we suggest that NN_5 could be associated with the lowest level ($\langle 200 \rangle$), provided a strong lattice distortion is involved.

Concerning NN_6 , the radiative efficiency is lower and two possibilities exist which should be equally discussed.

(i) Either we deal with an allowed pair and, in this case, NN_6 might correspond to any pair with C_s symmetry provided $c > a$ (for instance, $\langle 422 \rangle$, $\langle 622 \rangle$, $\langle 644 \rangle$) (it might also correspond to $\langle 400 \rangle$, provided a large lattice relaxation is involved), or

(ii) we deal with a forbidden pair; however, in this case, a large lattice relaxation should be involved in order to explain the radiative efficiency. As seen in Table III, the next forbidden pair which appears in the calculation is $\langle 112 \rangle$.

IV. DESCRIPTION OF LOCAL-FIELD SPLITTINGS OF Γ_8 BOUND HOLES

We want first to investigate, in light of the assignment previously discussed, the local-field effect experienced by

the Γ_8 bound hole. Experimental investigations have been conducted along this line in Ref. 19, and the magnitude of the local-field parameter (ϵ_1) has been obtained. It is interesting to note that ϵ_1 was found maximum for NN_2 but practically canceled for NN_5 and NN_6 . In this section, we show that we can identify and evaluate two explicit contributions to the uniaxial-field parameter ϵ_1 .

The bound-exciton wave function is taken in the Hartree approximation as $f(r_e)g(r_h)$, where $g(r_h)$ is an acceptorlike wave function centered at the midpoint 0 between the pair, and $f(r_e)$ is of the bonding type. In Ref. 22 it was shown that in zinc-blende semiconductors the acceptor ground state undergoes a splitting Δ when submitted to a perturbation $V(r)$:

$$\Delta = 4C_1C_2 \int V(r) \exp(-2r/a^*) [z^2 - \frac{1}{2}(x^2 + y^2)] d^3r, \quad (12)$$

where C_1 and C_2 are normalization coefficients of the Kohn-Schechter wave function and $a^* = 2/(a_1^{-1} + a_2^{-1})$; a_1 and a_2 are Bohr radii of this multicomponent wave function. It is obvious that a nonzero value of Δ is obtained if $V(r)$ has contributions of quadrupolar symmetry. In our problem, one can easily find two such contributions.

(i) The attractive potential of the electronic cloud corresponding to the bonding wave function $f(r_e)$.

(ii) The repulsive potential, of isoelectronic origin, which is produced by the two nitrogen atoms on the hole; let us remark that this component was hitherto neglected. Its sign, as well as its order of magnitude, can be obtained from the work of Harrison.²³

One can anticipate a possibility of cancellation between these two contributions of opposite signs. A third contribution related to the lattice strains caused by size mismatch is also present; however, for isolated N, it can be incorporated into the isoelectronic potential. For a pair, a contribution of lower symmetry might arise because strains would not add linearly; such terms are not evaluated in this paper.

The electronic wave function $f(r_e) = N[F(r_e - r_1) + F(r_e - r_2)]$ gives rise to a density of charge

$$N^2 [F(r_e - r_1)^2 + F(r_e - r_2)^2 + 2F(r_e - r_1)F(r_e - r_2)],$$

where $N^{-2} = 2(1 + O)$ and O is the overlap integral. We neglect the cross term on the grounds that it is rather centered around the midpoint 0. Then $V(r)$ in (12) is the sum of two equivalent parts V_1 and V_2 centered on each N atom; the integration in (12) can be done in the bipolar representation

$$\Delta = 8C_1C_2 \int V_2(r_2) \exp(-2r_1/a^*) [z^2 - \frac{1}{2}(x^2 + y^2)] \times r_1 r_2 R^{-1} dr_1 dr_2 d\psi, \quad (13)$$

where r_1 and r_2 are polar coordinates originating, respectively, from 0 and N atoms; R is the ON separation. After some algebraic manipulations one gets

$$\Delta = 16\pi C_1C_2/R \int_0^\infty dr_2 r_2 V_2(r_2) \times \int_{|R-r_2|}^{R+r_2} dr_1 r_1 \exp(-2r_1/a^*) \times Q(r_1, r_2), \quad (14)$$

where

$$Q(r_1, r_2) = 3R^2/8 + r_1^2/4 - 3r_2/4 + 3(r_1^2 - r_2^2)^2/(8R^2).$$

The integration over dr_1 can be performed analytically; then, the integration over dr_2 is done numerically.

Let us now discuss the choice of $V_2(r_2)$. For the isoelectronic potential, V_2 is just a constant in a sphere of radius r_0 . For the potential created by the electronic cloud, we proceed as follows: we assume that the shape of the electronic cloud depends mainly on the binding energy and on the effective mass of the electron. In the Hartree approximation, one can show that the wave functions of the electron are quite similar in NNX and in NN^- . On the other hand, it was shown in Sec. III that the NN^- problem in GaP was tricky because of the contributions of X , L , and Γ conduction bands, each NN configuration giving rise to specific interference effects. Considering that the weight of X and L valleys is preponderant and that average effective masses are comparable in these valleys ($\sim 0.6m_0$), we admit that for each NN configuration, the true system can be replaced by a single-valley semiconductor, where the depth of the isoelectronic potential (acting on the electron) has been adjusted in order to reproduce the experimental binding energy of NN^- ; We have used a square-well potential of radius $r_0 = 1.5 \text{ \AA}$ and the electrostatic potential V_2 is computed from the charge density by integration. Equation (14) has been evaluated for NN_1 to NN_7 using the pair configuration suggested from the results of uniaxial stress experiments combined with the theory of NN^- binding energy (see Sec. VII). A value $a^* = 12 \text{ \AA}$ was used. The results are summarized in Table IV. We have taken for the isoelectronic potential acting on the hole $V_h = 2.83 \text{ eV}$ in order to get an exact value for NN_4 (in that part, the isoelectronic potential acting on the electron is $V_e = -8.25 \text{ eV}$). Notice that this value of V_h is in the range of admissible values.

By inspection of Table IV, one can draw the following conclusions.

(i) The two perturbations we have computed indeed give sizable contributions to ϵ_1 .

(ii) With our choice of V_h , the net result has indeed the right order of magnitude and the positive sign of ϵ_1 is imposed by the perturbation of the nonspherical electron cloud.

(iii) The perturbation related to size mismatch, which we have neglected, decays rapidly with pair separation; very likely, it plays a significant role only for NN_2 and NN_1 .

(iv) For NN_6 we gave two possible assignments: $\langle 400 \rangle$ and $\langle 211 \rangle$. The comparison favors the second one.

V. HYDROSTATIC PRESSURE DEPENDENCE

We have already published a detailed investigation of the pressure dependence of N-related traps in GaP (Ref. 20). Striking results were obtained which demonstrated the great sensitivity of the binding energy to the lattice perturbations. Increasing the pressure, one expects the lattice constant to decrease. This should result in a deepening of the binding energy which is not found. In-

TABLE IV. Comparison of the theoretical and experimental values of the local-field parameter ϵ_1 which drives the splitting of the Γ_8 bound hole. The isoelectronic potential V_i , acting on the hole, has been adjusted to give an exact value for NN_4 . In the case of NN_6 , two possible assignments have been found. The comparison favors $\langle 211 \rangle$.

| Pair | Assignment | $2R$ (Å) | Δe | Δ_{ih} | ϵ_1 (theory) | ϵ_1 (expt.) |
|--------|-----------------------|-------------|------------|---------------|--------------------------|-------------------------|
| NN_1 | $\langle 220 \rangle$ | 7.71 | 0.8 | -0.7 | +0.1 | 0.3 |
| NN_2 | $\langle 110 \rangle$ | 3.85 | 0.184 | -0.224 | -0.04 | 0.45 |
| NN_3 | $\langle 442 \rangle$ | 16.35 | 2.5 | -1.6 | +0.9 | 0.20 |
| NN_4 | $\langle 440 \rangle$ | 15.42 | 1.71 | -1.49 | +0.22 | 0.22 |
| NN_5 | $\langle 200 \rangle$ | 5.45 | 0.2 | -0.4 | -0.2 | 0.07 |
| NN_6 | $\langle 211 \rangle$ | 6.67 | 0.3 | -0.5 | -0.2 | 0 |
| | $\langle 400 \rangle$ | 10.91 | 0.7 | -1.1 | -0.4 | 0 |
| NN_7 | $\langle 660 \rangle$ | 23.113 | 2.28 | -1.8 | +0.48 | 0.25 |

creasing the pressure, one finds the binding energy to decrease both for single-impurity bound excitons and pair levels. Identical results have been found independently by other workers.²⁴

Using a simple model of coupled quantum wells, this could be satisfactorily accounted for by renormalizing versus pressure the potential well associated with each nitrogen impurity. This was done in the form $V = V_0(1 + \epsilon)$, where a variation of ϵ versus pressure $d\epsilon/dP = -0.5\%$ per kbar around a mean value $\epsilon_0 = -0.08$ was shown to fit nicely the evolution of all binding energy from NN_1 to NN_∞ . Since we believe in a new ordering for the various pair levels, it is of interest to check how the evolutions under hydrostatic pressure are accounted for in the new model. Intuitively, under application of a hydrostatic pressure, two effects must happen. They should act again in an antagonistic manner on the bound states.

(i) The distance between the two N impurities decreases. This should result in a deepening of the level.

(ii) The lattice constant decreases. This dilates the Brillouin zone, moving the minima of the conduction band further apart in k space, and thus reduces the strength of the interferences. This should induce an uprise shift of the level. Indeed, this effect has been recently analyzed by Resca²⁵ in the framework of the effective-mass equation. He has shown, that with increasing pressure, the interval-

ley scattering factor $|\phi(r)|^2$ which multiplies the impurity potential $V(r)$ in his effective-mass formalism is scaled to a smaller region around the defect, which results in a lowering of the binding energy of the bound level.

Which of these effects is the dominant one can only be answered by performing a numerical calculation.

A. Details of the pressure-dependent calculation

Under application of a hydrostatic pressure, the conduction band deforms. Each Γ , X , and L minimum shifts with its own pressure coefficient C_i . When considering axial defects it is expected that the pressure coefficient depends upon the relative weights of the regions around Γ , X , and L and thus, in our model, varies differently according to the class of defects to which it belongs. In our numerical calculation, we first consider a linear variation of the lattice constant versus pressure:

$$a = a_0[1 + (S_{11} + 2S_{12})P].$$

(P is taken negative for a compression, and the coefficients S_{ij} have been taken from the literature.²⁶)

We also assume a linear shift of each minimum with pressure, with coefficients $C_X = -1.4$ meV/kbar, $C_L = 5.5$ meV/kbar, $C_\Gamma = 10.7$ meV/kbar, according to the work of Ref. 2. All results are listed in Table V for the

TABLE V. Calculated changes in electron binding energy (meV/kbar⁻¹) versus hydrostatic pressure. (a) takes only into account the change in nitrogen-nitrogen distance, (b) includes the change in band structure, (c) accounts also for the change in BZ, and lastly, (d) corresponds to theoretical values obtained by changing the nitrogen potential by -0.5% kbar⁻¹.

| Pair | Assignment | Theory | | | | Expt. ^a |
|--------|------------|--------|------|-------|------|--------------------|
| | | (a) | (b) | (c) | (d) | |
| NN_1 | 220 | 0.28 | -1.1 | -1.98 | -5.9 | -3.13 |
| NN_2 | 110 | 0.22 | -0.7 | -1.31 | -3.7 | -3.52 |
| NN_3 | 442 | 0.15 | -0.2 | -0.63 | -1.9 | -2.72 |
| NN_4 | 440 | 0.18 | -0.4 | -0.75 | -2.2 | -2.10 |
| NN_5 | 200 | 0.20 | -0.5 | -1.21 | -2.8 | -1.91 |
| NN_6 | 211 | 0.17 | -0.4 | -0.70 | -2.3 | -1.65 |
| NN_7 | 660 | 0.12 | -0.3 | -0.65 | -1.6 | -1.8 |

^a Reference 20.

NN_i pairs, together with the experimental values. Considering only the change in nitrogen-nitrogen distances, band-structure effects, and renormalization of the Brillouin zone, the signs and orders of magnitude are correctly reproduced (all levels more towards the conduction band), but the calculated values displayed in column (c) are systematically lower than the experimental ones. This difference cannot be attributed to the hole contribution which is one order of magnitude lower and must be ascribed to a change in potential experienced by the electron, originating most probably from the variation versus pressure of the local strain field surrounding the defect. In fact, it can be verified using an extended impurity potential that a local compression around each N atom results in a decrease of the equivalent one-site effective potential. This is best seen on Fig. 1. We show V_{eff}/V_0 for different strengths of the intersite first-neighbor interaction. Intuitively, one may think that the pressure will decrease the distance between each N atom and its surrounding neighbors, increasing the nondiagonal matrix elements V_{01} of the impurity potential and thus resulting in a delocalization of the electron. Taking a variation of these nondiagonal V_{01} matrix elements of the multisite SK potential of +7% per kbar is found in our model to be equivalent to a decrease of =0.5% for the one-site effective potential and results in a satisfactory agreement between the calculated and experimental variations of the binding energies, as can be seen in Table V.

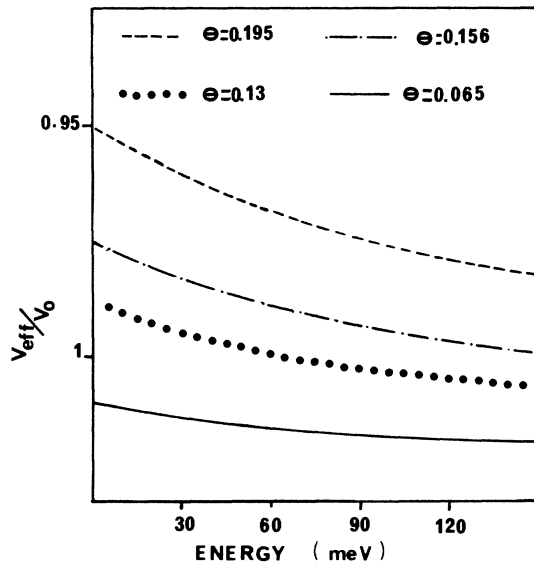


FIG. 1. Plot of the effective potential V_{eff} , in units of the "one-site" parameter of the Slater-Koster approximation (V_0) and for several values of the dimensionless parameter $\theta = V_{01}/V_{00}$. θ is the main parameter of the problem. It characterizes the strength of the isoelectronic potential in the real space around the impurity and equals zero in the one-site approximation. Given θ , V_{eff}/V_0 is an increasing function of the binding energy. At constant binding energy, V_{eff}/V_0 decreases versus θ when the delocalizations of both the wave function and the isoelectronic potential increase. Versus pressure, we expect θ to increase and the effective potential to decrease.

VI. DEPENDENCE OF LEVELS VERSUS COMPOSITION AND PRESSURE IN $\text{Ga}_x\text{In}_{1-x}\text{P}$ AND $\text{GaAs}_{1-x}\text{P}_x$

In the preceding sections we have shown that an easily tractable model calculation accounts satisfactorily for the physics of the nitrogen problem in GaP. This could be done by simply adjusting one matrix element which describes the nitrogen potential. Applying a hydrostatic pressure we have found that this matrix element varies. Again we could fit a complete series of data by simply adjusting the pressure dependence of our marginal potential. Since pressure and alloying have long been recognized to induce very similar effects, the question is to check the model versus composition.

A. $\text{Ga}_x\text{In}_{1-x}\text{P}$

This corresponds to the simple example of alloys where one substitutes only the cation. Assuming that the main effect of both pressure and alloying is to change the strength of the strain field surrounding the impurity, we can compute the composition dependence of the nitrogen level in $\text{Ga}_x\text{In}_{1-x}\text{P}$ from the change in lattice constant. Increasing the lattice constant increases the potential and results in the composition dependence shown in Fig. 2. We find a striking agreement with the experimental results of Ref. 27. The composition dependence of the conduction band which enters the calculation is obtained from the work of Ref. 28:

$$E_{\Gamma} = 1418 + 770x + 684x^2,$$

$$E_X = 2369 - 152x + 147x^2,$$

$$E_L = 2199 - 765x + 1204x^2,$$

where the position of the L_1 minimum in InP is obtained from Ref. 29. In order to perform a quantitative compar-

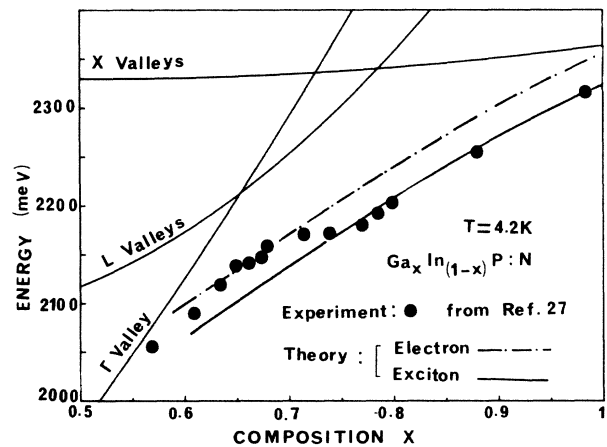


FIG. 2. Composition dependence of the nitrogen level in $\text{Ga}_x\text{In}_{1-x}\text{P}$. All experimental data are taken from the work of Ref. 27 and the band-structure variation versus composition is deduced from the work of Ref. 28. Notice that the electron-hole exchange and correlation effects shift the exciton by 33 meV with respect to the electron binding energy in the composition range $0.7 < x < 1$.

ison with experimental data (excitons), we account for the electron-hole exchange and correlation effects in a very simple way: we simply shift the electron energy line by 33 meV. [A correction of 33 meV makes a vanishingly small bound electron in GaP coincide with the experimental bound-exciton state (full line)]. This gives the theoretical exciton line, displayed as a solid line. It is interesting to notice that, depending on which minimum of the band structure appears lower, the agreement is best with (i) the exciton line in the range $0.7 < x < 1$, and (ii) the electron line in the range $x < 0.7$.

This can be qualitatively understood in light of a recent theoretical work. Considering a medium-range correlation potential, Jaros¹⁴ shows that the wave function associated with a weakly bound N^- electron state is intermediate between the strongly localized electron state given by the simple Slater-Koster model and the strongly delocalized one characteristic of standard hydrogenic donors. This is because the binding energy is mainly controlled by the stabilizing effect of the medium-range potential. However, it depends also on the properties of the lowest conduction band through a repulsive contribution. When going from GaP to InP, the lowest minimum changes from indirect to direct and the repulsive part of the binding energy increases. This makes the binding energy decrease to around ~ 0.7 .

B. GaAs_{1-x}P_x

Coming now to a more complicated situation, we investigate the nitrogen levels in GaAs_{1-x}P_x. This means that for composition x we substitute nitrogen to the virtual anion (As_{1-x}P_x). Considering the corresponding matrix element, one must take into account, first, the change in lattice constant. This is straightforward and has been done already in the case of Ga_{1-x}In_xP. Second, one must take into account the change in ionicity associated with the virtual anion. We have tentatively associated ionicity and atomic energy, and write

$$V_0(\text{GaAs}) = V_0(\text{GaP}) \frac{E_S(\text{N}) - E_S(\text{As})}{E_S(\text{N}) - E_S(\text{P})} \quad (15)$$

Taking all atomic energies as given by Harrison,²³ this gives in GaAs a resonant bound state of about 90 meV in the lowest conduction band which compares satisfactorily with the value deduced by Wolford *et al.*² by stimulating GaAs:N luminescence under hydrostatic pressure at 5 K ($80 < E_R < 120$ meV). We are now in a position to compute the change in electron binding energy versus composition on the full composition range. The results are displayed in Fig. 3 (dashed line). To favor a comparison with the experimental data of Ref. 2, a value of 33 meV is again assumed for the sum of exciton binding energy and electron-hole correlation effects and gives the "theoretical" exciton line (solid line). All values for the composition dependence of the conduction band are obtained from the work of Ref. 2. Obviously, the agreement between our computational work and the experimental data is very good and supports the model. Again we find that, depending on the details of the lowest conduction band, the agreement is better with the exciton line ($0.6 < X < 1$) or

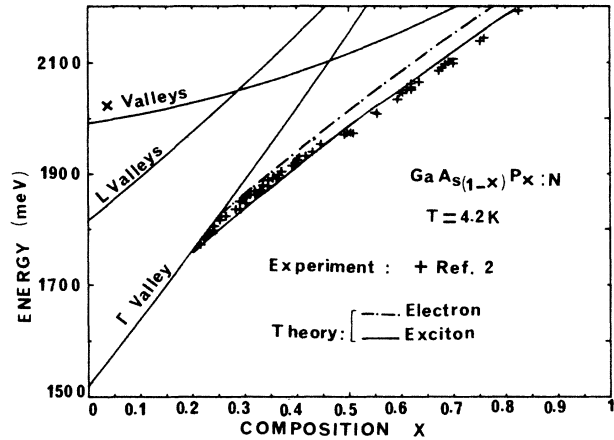


FIG. 3. Same as Fig. 4 but for GaAs_{1-x}P_x.

the electron line ($< 0.2 < X < 0.45$). Concerning NN pairs we find much fewer experimental results and concentrate on a very small range of composition near GaP (Ref. 30). Again the agreement is very good and shows that both the nitrogen potential we use and the band-structure parameters of Ref. 2 are very realistic. This is shown in Fig. 4. We emphasize that this approach is based on the virtual crystal approximation (VCA). When going to higher As concentrations, additional effects should be accounted for which come from a deviation from the standard Vegard law. The deviation is now well understood.³¹ The microscopic structure of pseudo-binary alloys is intermediate between the VCA and the pure ionic picture of Pauling and Huggins; the cation sublattice remains perfect and follows the Vegard law; on the contrary the anion sublattice relaxes to preserve the bond length of pure binary compounds. Since the local distortion mainly affects the anionic sublattice, these ef-

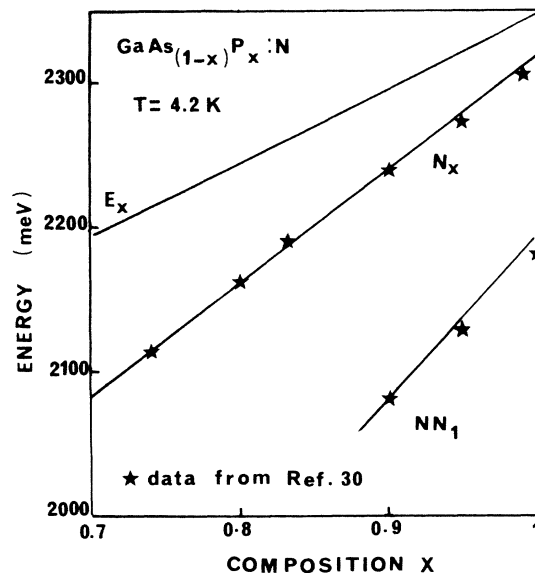


FIG. 4. Composition dependence of the NN₁ pair in GaAs_{1-x}P_x and comparison with experimental data of Ref. 30.

fects should not be missed when dealing with more extended ranges.

Since we have independently checked our calculation versus pressure in GaP and versus composition in $\text{Ga}_x\text{In}_{1-x}\text{P}$ and $\text{GaAs}_{1-x}\text{P}_x$, it is tempting to investigate what our predictions are using pressure on an alloy very close to GaAs. This corresponds with the experimental results of Ref. 2 on $\text{GaAs}_{0.957}\text{P}_{0.043}$ up to 60 kbar. Our theoretical findings are summarized in Fig. 5 and obviously agree very well with the experimental data.

VII. NITROGEN PROPERTIES IN GaAs

As already stated, nitrogen forms a resonant bound state in GaAs which emerges from the continuum of the conduction band around 22 kbar.² At $P=0$, the corresponding eigenstate mainly depends on the electronegativity difference between arsenic and nitrogen and a crude estimate could be obtained, assuming that the change in electronegativity just reflects the change in atomic energies. A resonant bound state was found at 92 meV above the lowest minimum of the conduction band (see Sec. VI B) which is a very reasonable value and which reinforces the model.

On the other hand, recent investigations of the pressure dependence of shallow bound states in GaAs have been conducted^{32,33} and detailed information about the pressure dependence of the band structure has been obtained.³² In the light of these new results, we are in a position to reinvestigate very accurately the energy position of the nitrogen resonant state in GaAs. We take experimental pres-

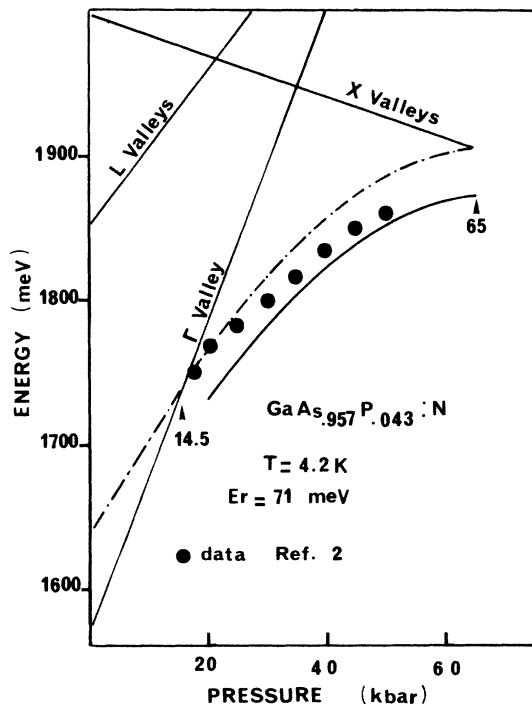


FIG. 5. Pressure dependence of nitrogen-bound excitons in $\text{GaAs}_{0.957}\text{P}_{0.043}$. Experimental results are from Ref. 2.

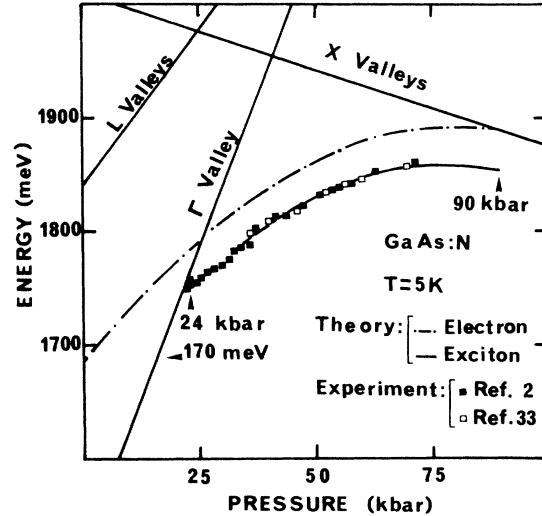


FIG. 6. Pressure dependence of nitrogen states in GaAs. The solid line is computed with $V_0=2.112$ eV and $(1/V_0)(dV_0/dp)=-1.55\%$ per kbar⁻¹. We assume a constant energy of 33 meV for exchange and correlation effect. The resonant bound state is found at 1690 meV under atmospheric pressure conditions. Experimental results at 5 K are from Wolford *et al.* (Ref. 2) and M. Leroux (Ref. 33).

sure coefficients ($dE_\Gamma/dP=10.73$ meV/kbar, $dE_L/dP=5.5$ meV/kbar, and $dE_X/dP=-1.34$ meV/kbar) together with energy differences [$E(X_1)=2010$ meV and $E(L_1)=1840$ meV] from the work of Ref. 32 and slightly adjust our matrix element (V_0) and pressure dependence (dV_0/dP) in order to get the best overall agreement. The results have been displayed in Fig. 6. We find a resonant state in GaAs lying 170 meV above the Γ_{1c} minimum of the conduction band which, under hydrostatic pressure, forms in the gap at 24 kbar. Increasing the pressure, the binding energy first increases up to 41.5 kbar and then starts to decrease. The bound electron should ionize at 90 kbar, which corresponds to the experimental situation encountered in GaP under atmospheric pressure conditions.

VIII. CONCLUSION

We have presented a model calculation of nitrogen bound states in GaP and related compounds. This calculation was voluntarily restricted to the one-band-one-site approximation in order to give meaningful results. Taking full account of the indirect structure of the lowest conduction band, it allowed a satisfactory comparison with previously published results and permitted us to discuss the assignment of NN levels. In light of this new proposal, we could discuss up to NN_7 the hydrostatic stress dependence of the bound-exciton complex and the local-field splitting experienced by the Γ_8 bound hole.

Considering next the change in nitrogen potential associated with the formation of Ga-X-P alloys ($X=\text{In,As}$), we got satisfactorily data for the composition dependence of the nitrogen bound state. We emphasize again that this result is obtained over the full composition range without the help of any additional parameter. When substituting

the cation ($X=\text{In}$), the change in nitrogen potential is only driven by the change in lattice parameter surrounding the defect. On the contrary, when substituting the anion, both the change in lattice parameter and ionicity must be taken into consideration. This gives a resonant state in GaAs located ~ 100 meV above the Γ_{1c} conduction-band minimum. Again this is in satisfactory agreement with the experimental data. When changing now the hydrostatic pressure, we change only the lattice parameter and again compute data in very satisfactory agreement with the experimental results.

To summarize, we have presented a very simple calculation of nitrogen properties in GaP and related compounds, which satisfactorily accounts for all existing data. Applying this calculation to the problem of nitrogen-nitrogen pairs, we have discussed a possible ordering which differs from the conventional one. This ordering takes into account the local symmetry of NN traps.

Note added in proof.

Since the completion of this work, we have been aware of the results of a new calculation that has been published [Phys. Rev. B 22, 6907 (1985)]. The calculation assumes a defect potential described by two parameters V_s and V_p and the host band structure is obtained from a ten-states linear combination of atomic orbitals. Working in the framework of the assignment given by Thomas and Hopfield, with electron energies deduced from the work of Cohen and Sturge,¹⁰ the authors use V_p to adjust the family of $\langle 110 \rangle$ pairs at an energy of 120 meV (NN_1). Next V_s determines the whole series of levels from NN_2 to NN_7 . They find again an ordering at variance with the standard assignment but their proposal does not agree with our experimental symmetries.

Although one must be very cautious in discussing the results of various theoretical calculations, this work questions the existence of the interference effects discussed in this work and already noticed by Faulkner⁵ or Brand and Jaros.⁶ One explanation might be the poor representation of the density of states in the conduction band obtained in the scheme of Hjalmarson *et al.*¹³ by artificially lowering the X point by means of excited S^* states. In fact, one must remember that the same type of Green's function calculation performed with a ten-bands Hamiltonian by Brand and Jaros shows that the interference effects do exist due to the proximity of the lowest conduction band to the NN^- bound states.

APPENDIX

The model used to describe the lowest conduction band in GaP has been already discussed by G. G. Kleiman¹⁷ and then used extensively in the studies of single nitrogen impurities in GaP and $\text{GaAs}_{1-x}\text{P}_x$. According to this model the Brillouin zone is divided in regions associated with the Γ , X , and L minima. Around each nonequivalent minimum $k_{i,1}$ of type i ($i=\Gamma, X, L$), the energy dispersion is taken as parabolic with finite extension:

$$E_c(\mathbf{k}) = E_c(\mathbf{k}_i + \mathbf{q}) = E_i + \alpha_i q^2,$$

where E_i denotes the energy at the minimum of interest and $q < k_i^m$. α_i is directly related to the effective mass m_i^* at $\mathbf{k}_{i,1}$: $\alpha_i = \hbar^2/2m_i^*$. Here we have taken isotropic effective masses

$$m_{\Gamma}^*/m_0 = 0.12, \quad m_L^*/m_0 = 0.298, \quad m_X^*/m_0 = 0.36,$$

where m_0 is the free-electron effective mass.

The "cutoff" k_i^m momenta, which determine the relative weights of each region surrounding the critical point, have been attributed to the same values as the ones obtained by Kleiman¹⁷ by requiring that the total number of states in each region be equal to the one determined by pseudopotential densities of states. These values are, respectively,

$$k_{\Gamma}^m a = 0.974, \quad k_X^m a = 3.898, \quad k_L^m a = 2.443,$$

where a is the lattice constant; $a = 5.45 \text{ \AA}$ in GaP.

Using this partition of the Brillouin zone, the Green's function

$$G_c(\epsilon, \mathbf{R}) = \frac{\Omega}{(2\pi)^3} \int_{\text{BZ}} \frac{e^{i\mathbf{k}\cdot\mathbf{R}}}{\epsilon - E_c(k)} d^3k$$

can then be easily shown to be given as

$$G_c(\epsilon, \mathbf{R}) = \sum_i f_i(\mathbf{R}) g_i(\epsilon, \mathbf{R}),$$

where

$$f_i(\mathbf{R}) = \sum_{l \in i} e^{i\mathbf{k}_l \cdot \mathbf{R}}$$

and

$$g_i(\epsilon, \mathbf{R}) = -\frac{\Omega}{2\pi^2 \alpha_i R} \int_0^{K_i^m} \frac{q \sin(qR)}{q_0^2 + q^2} dq.$$

$q_0 = (\epsilon - E_i/\alpha_i)^{1/2}$ and $\Omega = a^3/4$ is the unit-cell volume. In the particular case $R = 0$,

$$G_c(\epsilon) = \frac{\Omega}{(2\pi)^3} \int_{\text{BZ}} \frac{d^3k}{\epsilon - E_c(k)}$$

is obtained as

$$G_c(\epsilon) = \sum_i n_i g_i(\epsilon),$$

where n_i is the number of inequivalent minima of each type ($n_{\Gamma} = 1$, $n_X = 3$, $n_L = 4$) and $g_i(E)$ is obtained as

$$g_i(E) = -\frac{\Omega}{2\pi^2 \alpha_i} \left[K_i^m - q_0 \arctan \left[\frac{K_i^m}{q_0} \right] \right].$$

In GaP the relative energies of the Γ and L minima with respect to the lowest X have been taken as

$$E_{\Gamma} = 530 \text{ meV}$$

and

$$E_L = 395 \text{ meV}.$$

- ¹D. G. Thomas and J. J. Hopfield, *Phys. Rev.* **150**, 680 (1966).
- ²D. J. Wolford, J. A. Bradley, K. Fry, J. Thompson, and H. E. King, *Inst. Phys. Conf. Ser.* **65**, 477 (1983); also see *Proceedings of the International Conference on the Physics of Semiconductors, San Francisco, 1984*, edited by J. D. Chadi and W. A. Harrison (Springer, New York, 1985), p. 627.
- ³W. T. Masselink and Ya-Chung Chang, *Phys. Rev. Lett.* **51**, 509 (1983).
- ⁴C. Benoit à la Guillaume, *Physica* **117-188B**, 105 (1983); also see *J. Phys. (Paris) Lett.* **44**, L53 (1983).
- ⁵R. A. Faulkner, *Phys. Rev.* **175**, 991 (1968).
- ⁶S. Brand and M. Jaros, *J. Phys. C* **12**, 2789 (1979); see also M. Jaros and S. Brand, *ibid.* **12**, 525 (1979).
- ⁷B. Gil, J. Camassel, J. P. Albert, and H. Mathieu, preceding paper, *Phys. Rev. B* **33**, 2690 (1986).
- ⁸See, for instance, W. Czaja, *Festkoerperprobleme* **11**, 65 (1971).
- ⁹J. J. Hopfield, D. G. Thomas, R. T. Lynch, *Phys. Rev. Lett.* **17**, 312 (1966).
- ¹⁰E. Cohen and M. D. Sturge, *Phys. Rev. B* **15**, 1039 (1977).
- ¹¹J. C. Philipps, *Phys. Rev. Lett.* **22**, 285 (1968).
- ¹²J. W. Allen, *J. Phys. C* **4**, 1936 (1971).
- ¹³H. P. Hjalmarson, P. Vogl, D. J. Wolford, and J. D. Dow, *Phys. Rev. Lett.* **44**, 810 (1980).
- ¹⁴M. Jaros, *Solid State Commun.* **51**, 411 (1984).
- ¹⁵J. Bourgoin and M. Lannoo, *Point defects in Semiconductors* (Springer, Berlin, 1983).
- ¹⁶W. Y. Hsu, J. D. Dow, D. J. Wolford, and B. G. Streetman, *Phys. Rev. B* **16**, 1597 (1977).
- ¹⁷G. G. Kleiman, *Phys. Rev. B* **6**, 3198 (1979).
- ¹⁸L. Resca and R. Resta, *Solid State Commun.* **29**, 275 (1979); *Phys. Rev. Lett.* **44**, 1340 (1980); M. Altarelli and W. Y. Hsu, *ibid.* **43**, 1346 (1979).
- ¹⁹B. Gil, J. Camassel, P. Merle, and H. Mathieu, *Phys. Rev. B* **25**, 3987 (1982).
- ²⁰B. Gil, M. Baj, J. Camassel, H. Mathieu, C. Benoit à la Guillaume, N. Mestres, and J. Pascual, *Phys. Rev. B* **29**, 3398 (1984).
- ²¹M. Mariette, J. Chevalier, and P. Leroux-Hugon, *Phys. Rev. B* **21**, 5706 (1980).
- ²²C. Benoit à la Guillaume, *Solid State Commun.* **48**, 513 (1983).
- ²³W. A. Harrison, *Electronic Structure and the Properties of Solids* (Freeman, San Francisco, 1980), see table 10-1, p. 253.
- ²⁴X. R. Zao, G. H. Lee, H. X. Han, Z. P. Wang, R. M. Tan, and J. Z. Hu, *Acta Phys. Sin.* **33**, 583 (1984).
- ²⁵L. Resca, *Phys. Rev. B* **29**, 866 (1984).
- ²⁶W. Boyle and R. J. Sladek, *Phys. Rev. B* **11**, 2933 (1975).
- ²⁷J. Chevalier, *J. Phys. C* **3**, 207 (1974).
- ²⁸P. Merle, D. Auvergne, H. Mathieu, and J. Chevalier, *Phys. Rev. B* **15**, 2032 (1977).
- ²⁹Chelikowski, J. Chadi, and M. H. Cohen, *Phys. Rev. B* **8**, 2786 (1973).
- ³⁰M. Mariette, Thesis, Université P. et M. Curie, Paris, 1981.
- ³¹P. Bogulawski and A. Baldereschi, in *Proceedings of the 17th International Conference on the Physics of Semiconductors, San Francisco, 1984* (Springer, New York, 1985), p. 939; J. C. Mikkelsen, Jr. and J. B. Boyce, *Phys. Rev. B* **28**, 7130 (1983).
- ³²D. J. Wolford and J. A. Bradley, *Solid State Commun.* **53**, 1069 (1985).
- ³³M. Leroux (unpublished).